

Relaxation Dynamics in the Spin-1 Heisenberg Antiferromagnetic Chain after a Quantum Quench of the Uniaxial Anisotropy

D. WOŹNIAK^a, A. DRZEWIŃSKI^{a,*} AND G. KAMIENIARZ^b

^aInstitute of Physics, University of Zielona Góra, Prof. Z. Szafrana 4a, 65-516 Zielona Góra, Poland

^bFaculty of Physics, A. Mickiewicz University, Umultowska 85, PL-61614 Poznań, Poland

(Received February 26, 2016; in final form November 3, 2016)

In the framework of the matrix product state representation the effect of a sudden turning on of the uniaxial anisotropy on the time evolution of the Haldane state has been investigated. Depending on the value of the uniaxial anisotropy parameter, the calculations were derived within (or outside) the region where the Haldane gap survives. An exact expression for the time evolution of the Loschmidt echo has been derived and, moreover, its collapse and revival behaviour was captured. In addition, the non-local order parameter of a time evolving state was tracked, revealing two types of relaxations.

DOI: [10.12693/APhysPolA.130.1395](https://doi.org/10.12693/APhysPolA.130.1395)

PACS/topics: 75.10.Jm, 76.60.Es, 05.30.-d, 75.30.Gw

1. Introduction

Above the range of very low temperatures many magnetic systems can demonstrate a quasi one-dimensional (1D) behaviour. Moreover, the magnetic properties of many compounds available for experiments are related to antiferromagnetic spin chains. In the investigation of the antiferromagnetic Heisenberg model, the chain of $S = 1/2$ spins was first solved by means of the Bethe ansatz in 1931 [1]. The ground state has no energy gap to the excited states accompanied by the exponential decay of the spin-spin correlations with distance. Although initially the concept of the 1D magnetism was considered as only theoretical, magnetic materials showing such a behaviour were found in the 70's [2]. This was of great importance because of the effects associated with quantum correlations and fluctuations, which are particularly exposed in the 1D spin systems.

Since the dispersion of the elementary excitation spectrum for half-integer spin chains was as for the classical spin waves, it was implied that the behaviour of the Heisenberg model with larger spins smoothly converges to the classical case. It thus came as a surprise when Haldane conjectured in 1983 that quantum Heisenberg antiferromagnetic chains have qualitatively different properties according to whether the spin value is integer or half-integer [3].

In recent years, cold atoms have been widely used in advanced research to mimic phenomena in condensed matter physics [4, 5]. They are placed into optical lattices providing a periodic potential without defects and phonon excitations. As a result, cold atoms and ions allow for practically perfect realizations of spin models [6, 7]. The comparison of the properties of integer

and half-integer spin chains may be realized with trapped ultra-cold atomic gases [7]. It opens the experimental way to investigate the dynamical properties of the Haldane state [8, 9] and gives the motivation for our theoretical research.

In this paper we focus on the time evolution of the Haldane system after a global quantum quench of the D uniaxial anisotropy. It corresponds to an experimental situation, in which a global parameter has been changed on a time scale smaller than the time scale of any system process. As the Haldane state is overlapped with many eigenstates of the nonzero- D Hamiltonian it can lead to nontrivial dynamics. Furthermore, one can expect that the value of the anisotropy constant affects the relaxation dynamics.

The paper is organized as follows: in Sect. 2 the model to study dynamics of the disturbed Haldane state is defined, Sect. 3 presents the matrix product state (MPS) formalism employed for time evolution simulations, whereas the simulation results are discussed in Sect. 4. Finally, Sect. 5 concludes our paper, summarizing the main findings.

2. Model

In order to study the ground-state dynamics we have considered the quantum chain with $N = 102$ sites and open boundary conditions. Two other spin chains with a length of $N = 4$ and $N = 10$, which can be solved by exact numerical methods, constitute a point of reference for our considerations.

2.1. The vanishing uniaxial anisotropy

The $S = 1$ antiferromagnetic Heisenberg chain is governed by the following Hamiltonian:

$$\mathcal{H}_J = J \sum_{i=1}^{N-1} S_i^x S_{i+1}^x + S_i^y S_{i+1}^y + S_i^z S_{i+1}^z, \quad (1)$$

*corresponding author; e-mail: A.Drzewinski@if.uz.zgora.pl

where the parameter $J > 0$ is an exchange coupling constant. It is known that to construct the ground state of the Hamiltonian (Eq. (1)) each original $S = 1$ spin can be written as two $S = 1/2$ spins in the triplet state. Based on them the ground state (the so-called valence-bond-state) can be built [10, 11]. However, when we are dealing with an open chain, both $S = 1$ spins at the ends can be replaced by the $S = 1/2$ spins to keep unchanged a nonzero energy gap between the singlet ground state $|\psi_0\rangle$ and the first excited state [10, 12, 13]. The ground-state energy per spin is $E \approx -1.40$ J and the excitation spectrum has a gap $\Delta \approx 0.41$ J [14].

Besides exhibiting the famed Haldane gap, the $S = 1$ antiferromagnetic Heisenberg chain has been found to have other surprising features. At first, due to the existence of a finite energy gap above the ground state, the spin-spin correlations $C_{j,k}^\alpha$ ($\alpha = x, y, z$) should decay exponentially

$$C_{j,k}^\alpha = (-1)^{k-j} \langle S_j^\alpha S_k^\alpha \rangle. \quad (2)$$

Recently another basic property of the Haldane phase in spin-1 Heisenberg antiferromagnetic chains has been brought: the eigenvalues of the reduced density matrix are always in even multiplets [15]. Moreover, the Haldane phase, as a topologically protected phase in one dimension, does not obey the Landau paradigm [16] and cannot be characterized by a local order parameter. But a nonlocal hidden order can be characterized by the antiferromagnetic alignment of ± 1 spins after omitting all the sites with spin projection 0. It was consistent with a breaking of a hidden $Z_2 \times Z_2$ symmetry, which was revealed using a nonlocal unitary transformation by Kennedy and Tasaki [17]. It leads to the existence of the non-local order parameter O^α ($\alpha = x, y, z$) that should be nonzero in the Haldane phase [18], where the Néel order vanishes. It is defined by the non-local correlation functions $O_{j,k}^\alpha$ in the following way:

$$O^\alpha = \lim_{|j-k| \rightarrow \infty} \langle O_{j,k}^\alpha \rangle \neq 0, \quad (3)$$

where

$$O_{j,k}^\alpha = S_j^\alpha \otimes e^{i\pi S_{j+1}} \otimes e^{i\pi S_{j+2}} \otimes \dots \otimes e^{i\pi S_{k-1}} \otimes S_k^\alpha. \quad (4)$$

2.2. The non-zero uniaxial anisotropy

In real materials the uniaxial anisotropy can be created through the environment of the magnetic ion [19–21] which implies adding the extra term to the Hamiltonian (Eq. (1)):

$$\mathcal{H}_D = D \sum_{i=1}^N (S_i^z)^2, \quad (5)$$

where D is the uniaxial anisotropy parameter which describes the system with an easy axis (negative D) or an easy plane (positive D). The Haldane gap persists in the presence of the $D/|J|$ parameter between ≈ -0.315 and ≈ 0.968 [19, 22–26], so the calculation was performed for the following values: $D/|J| = -1.0, -0.1, 0.5, 1.5$.

The large D phase is established for the $D/|J| > 0.968$ and the transition separating the Haldane and large

D phases is Gaussian. The Gaussian transition in the $S = 1$ chain is topological, in that the parity of the ground state changes from negative in the Haldane phase to positive in the large- D phase. The Haldane gap vanishes at the critical value of $D/|J| = 0.968$ but increases again afterwards, which primarily is related to the large value of D . In the large D phase, the ground state is given by a single tensor product of local states where all spins are restricted to the $S_i^z = 0$ state.

Between the Haldane and Néel phases at $D/|J| < -0.315$ there is the second-order Ising transition [27]. In the Néel phase the ground state exhibits a spontaneous staggered magnetization. The result is that the non-local order parameter identifying the Haldane phase, is also non-zero here. However in this case, contrary to the Haldane phase, the non-local order parameters $O^{x,y}$ decay exponentially.

2.3. The ground-state overlap

The overlap between the zero- D ground state and the ground-states for a non-zero uniaxial anisotropy has been considered. As the total spin operator commutes with the Hamiltonian (Eq. (1)) with and without the anisotropic term (Eq. (5)), both the ground states belong to the subspace with total spin $S^z = 0$.

The results are collected in Fig. 1. As shown, when the chain is short, the scalar product decreases slowly with increasing amplitude of the D parameter. However, when the system size increases, the range of the D parameter giving the nonvanishing scalar product, more and more overlaps with the range of the D parameter for which the Haldane gap is not closed for the infinite system.

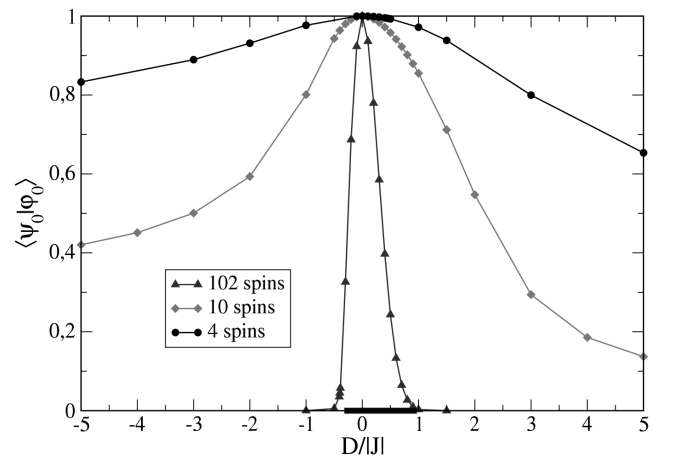


Fig. 1. The overlap of the initial ground-state function $|\psi_0\rangle$ with the ground-state functions $|\phi_0\rangle$ for non-zero uniaxial anisotropy. The thick black section denotes the Haldane regime for the infinite system.

3. Time evolution of matrix product states

In order to investigate the ground state and its dynamical properties after a sudden change of the Hamiltonian parameters the MPS formalism has been employed [28, 29]. The observation that for physical systems

only minor part of the Hilbert space is involved [30], resulted in the rapid development of numerical methods based on a variational method within the space of MPS. It corresponds to assigning a finite entanglement content to spins in the ground state. Therefore, any state of the spin chain can be presented in the MPS representation

$$|\psi\rangle = \sum_{\sigma_1, \dots, \sigma_N} \sum_{d_1, \dots, d_{N-1}} M_{1, a_1}^{\sigma_1} M_{a_1, a_2}^{\sigma_2} \dots M_{a_{N-1}, 1}^{\sigma_N} |\sigma\rangle, \quad (6)$$

where $|\sigma\rangle = |\sigma_1, \dots, \sigma_N\rangle$, d_j is the dimension of the local base $\{\sigma_j\}$ at the i -th site, whereas D_j are related to the entanglement of neighbouring spins. In an analogous manner any operator \mathcal{A} can be written as a matrix product operator (MPO):

$$\mathcal{A} = \sum_{\sigma_1, \dots, \sigma_N} \sum_{\sigma'_1, \dots, \sigma'_N} W^{\sigma_1 \sigma'_1} W^{\sigma_2 \sigma'_2} \dots W^{\sigma_N \sigma'_N} |\sigma\rangle \langle \sigma'|. \quad (7)$$

Due to the above representation the state space grows only polynomially in the system size (not exponentially as usual). Thus, the time of calculations is significantly reduced for $d = 1$ strongly correlated systems. When the variational principle is applied, the ground state can be found by the minimization procedure $\langle \psi | \mathcal{H} | \psi \rangle$ under the constraint $\langle \psi | \psi \rangle = 1$ [31]. Moreover, it is one of the most attractive features of the MPS representation that the time evolution can also be performed very efficiently. Therefore, discrete time as $t = N\Delta t$ can be used for the Hamiltonian, when a second-order Trotter decomposition is applied [29] the time-evolution operator can be presented as

$$e^{-i\mathcal{H}\Delta t} = e^{-i\mathcal{H}_o\Delta t/2} e^{-i\mathcal{H}_e\Delta t} e^{-i\mathcal{H}_o\Delta t/2} + O(\Delta t^3), \quad (8)$$

where

$$\mathcal{H}_o = J \sum_{i=1}^{N/2} S_{2i-1}^x S_{2i}^x + S_{2i-1}^y S_{2i}^y + S_{2i-1}^z S_{2i}^z, \quad (9)$$

$$\mathcal{H}_e = J \sum_{i=1}^{N/2-1} S_{2i}^x S_{2i+1}^x + S_{2i}^y S_{2i+1}^y + S_{2i}^z S_{2i+1}^z + D \sum_{i=1}^N (S_i^z)^2. \quad (10)$$

Then the time-evolution algorithm takes a very simple form [28]: one starts from $|\psi_0\rangle$ and repeats the following steps:

1. Applying the MPO of the odd bonds to $|\psi(t)\rangle$.
2. Applying the MPO of the even bonds to $e^{-i\mathcal{H}_o\Delta t/2} |\psi(t)\rangle$.
3. Applying the MPO of the odd bonds to $e^{-i\mathcal{H}_e\Delta t} e^{-i\mathcal{H}_o\Delta t/2} |\psi(t)\rangle$.
4. Compressing the MPS $|\psi(t + \Delta t)\rangle = e^{-i\mathcal{H}_o\Delta t/2} e^{-i\mathcal{H}_e\Delta t} e^{-i\mathcal{H}_o\Delta t/2} |\psi(t)\rangle$ to the starting dimension.

In the present studies the maximal local bond dimension was $D_i = 120$, whereas the time step was $\Delta t = 10^{-5}$.

4. The Loschmidt echo

The stability of quantum systems to perturbations of the Hamiltonian has been addressed by many studies [32]. It is relevant for fundamental research into the thermalization of isolated quantum systems [33], localization phenomena, chaos [34, 35], or decoherence.

As for both Hamiltonians \mathcal{H}_J and $\mathcal{H} = \mathcal{H}_J + \mathcal{H}_D$ the total spin is conserved, we can exploit this symmetry to reduce the computational effort. Let us assume that the initial state $|\psi_0\rangle$ is the ground state of the Hamiltonian \mathcal{H}_J (Eq. (1)) belonging to its zero total spin subspace. For $t > 0$ the time evolution is governed by the anisotropic Hamiltonian \mathcal{H} and the $|\psi_0\rangle$ state is never more its eigenstate. Nonetheless, the time evolution of the initial state

$$|\psi(t)\rangle = e^{-i\mathcal{H}t} |\psi_0\rangle \quad (11)$$

takes place in the anisotropic Hamiltonian subspace again corresponding to total spin zero. In order to measure the overlap of the time-evolved state and the initial state we can use, so-called, the Loschmidt echo (also called ‘‘quantum fidelity’’ commonly applied in the fields of quantum information and quantum chaos [36]) defined as [37]:

$$L(t) = |\langle \psi_0 | \psi(t) \rangle|^2 = |\langle \psi_0 | e^{-i\mathcal{H}t} | \psi_0 \rangle|^2. \quad (12)$$

If $|\phi_j\rangle$ and E_j are the eigenstates and eigenvalues of the new Hamiltonian, i.e., $(H_J + H_D)|\phi_j\rangle = E_j|\phi_j\rangle$, the initial state $|\psi_0\rangle$ can be expressed as a linear combination of the new stationary states $|\psi_0\rangle = \sum_{j=0}^{n-1} c_j |\phi_j\rangle$ where the coefficients are defined as $c_j = \langle \phi_j | \psi_0 \rangle$. This expansion enables us to rewrite the Loschmidt echo in the following way:

$$L(t) = |c_0|^2 + \sum_{k=1}^{n-1} |c_k|^2 \exp(-i(E_k - E_0)t)^2, \quad (13)$$

where E_0 is the ground-state energy of the new Hamiltonian. Next, repeatedly using the de Moivre formula and Pythagorean trigonometric identity the formula can be simplified to the final form

$$L(t) = \sum_{k=0}^{n-1} |c_k|^4 + \sum_{j>k}^{n-1} |c_j|^2 |c_k|^2 \cos((E_k - E_j)t). \quad (14)$$

Figures 2–4 present the time evolution of the Loschmidt echo after a rapid turning on of the uniaxial anisotropy for the Haldane system of different lengths. Because for the shortest chain the Haldane phase is smeared out significantly, two curves in Fig. 2 were made for higher values of the anisotropy parameter than usual: $D/|J| = -10$ instead of -1 and $D/|J| = 5$ instead of 1.5 .

In all cases the echo behaviour can be explained by Eq. (14): there is a constant contribution from the sum of the fourth powers of the coefficients supplemented by a superposition of cosine functions. When the system is very small, as in Fig. 2, the number of cosine functions is notably reduced. For example, in this case, although the subspace of total spin $S^z = 0$ is ten-dimensional, for each value of anisotropy only four coefficients are non-vanishing. For the $N = 10$ chain the subspace of

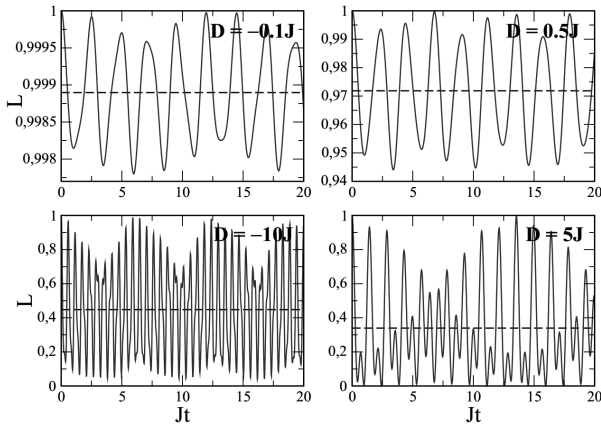


Fig. 2. The time evolution of the Loschmidt echo for the $1/2-1-1-1/2$ chain. The dashed lines mark a contribution from the sum of the fourth powers of the c_j coefficients.

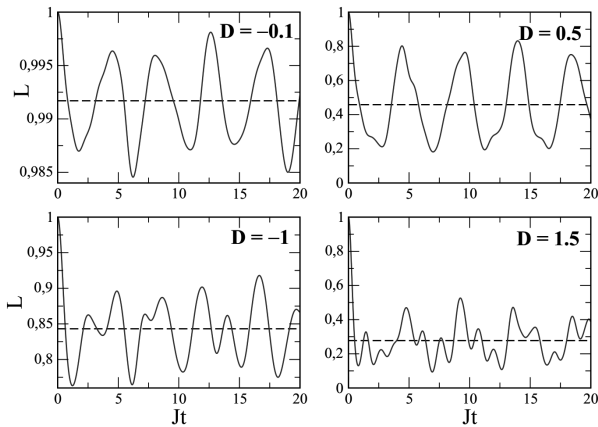


Fig. 3. The time evolution of the Loschmidt echo for the $1/2-1-1-1-1-1-1-1/2$ chain. The dashed lines mark a contribution from the sum of the fourth powers of the c_j coefficients.

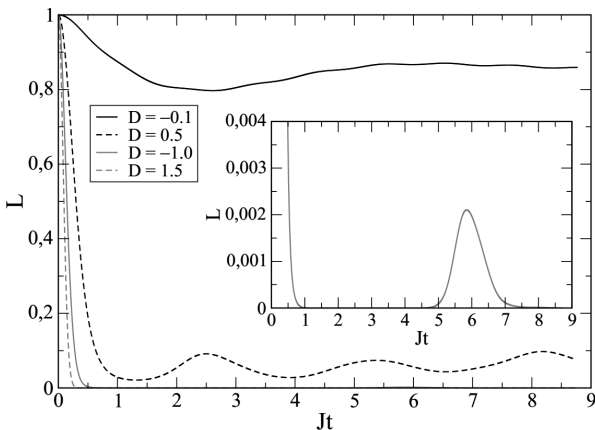


Fig. 4. The time evolution of the Loschmidt echo for the spin-1 chain ($N = 102$ including the $S = 1/2$ edge spins). The figure includes cases related to the Haldane phase ($D/|J| = -0.1$ and 0.5), the Néel phase ($D/|J| = -1$) and large- D phase (1.5). Inset: the short-term revival of the Loschmidt echo in the Néel state.

total spin $S^z = 0$ is 4246-dimensional and again the number of non-vanishing coefficients is considerably reduced. Moreover, the more parameter D deviates from zero, the greater the number of non-zero coefficients: 1112 for $D/|J| = 0.1$, 1150 for $D/|J| = -0.5$, 1303 for $D/|J| = 1.0$, and 1364 for $D/|J| = -1.5$.

When the system is large (see Fig. 4), the Loschmidt echo as usual converges to a constant value. But now, despite a significant reduction of non-vanishing coefficients their number is enormous. Furthermore, for a large system one can notice an important regularity related to the distribution of coefficient values. When the D value deviates not much from zero (see Fig. 1), which occurs in the Haldane phase, the coefficient c_0 dominates ($c_0 \approx 0.923$ for $D/|J| = 0.1$ and $c_0 \approx 0.243$ for $D/|J| = -0.5$) and the role of the constant term is crucial. In contrast, when one goes beyond the Haldane phase, the c_0 coefficient is very small ($c_0 \approx 8 \times 10^{-6}$ for $D/|J| = 1.0$ and $c_0 \approx 3 \times 10^{-7}$ for $D/|J| = -1.5$). Then the distribution of all coefficients becomes more balanced and the constant term takes a very small value of the order 10^{-6} for $D/|J| = 1.0$ and of the order 10^{-9} for $D/|J| = -1.5$.

At the beginning of the time evolution, as one can see, the decay of the Loschmidt echo is monotonic. Furthermore, it is known from the standard perturbation theory that the initial time decay of the Loschmidt echo exhibits a Gaussian decay when the perturbation is weak [38, 39]. As we have verified, regardless of the value of the anisotropy parameter, for small Jt all curves presented in Fig. 4 demonstrate such behaviour $L(Jt) \sim \exp(-\gamma \times (Jt)^2)$ where the rate of the exponential decay is proportional to the second power of the anisotropy parameter $\gamma \sim D^2$. As can be seen from Eq. (14), from time to time such a superposition of cosine functions can be expected when the echo value increases significantly. The time after which the full restoration of the initial Loschmidt echo takes place is likely to be hideously large but other peaks of the Loschmidt echo should be available for our simulation. One of them is demonstrated in the inset of Fig. 4 where the significant revival of the Loschmidt echo appears in the presence of the seemingly vanishing background.

5. Non-local correlations in the Haldane phase

The initial state (the Haldane state) is isotropic in the spin space, so all the components are the same at $t = 0$. After a sudden turning on of the uniaxial anisotropy the x, y components behave differently than the z component. To minimize edge effects in a finite system the spins in pairs were chosen so that they are separated by a distance $2k - 1$ arranged symmetrically relative to the chain center. As we have checked, regardless of the value of the uniaxial anisotropy, the Néel correlation functions decay exponentially during the whole time evolution.

The non-local order reflects the hidden symmetry in the Haldane phase. Previously, we have examined that the string correlation functions for the established ground state of \mathcal{H}_J show a wide plateau followed by a gradual decline as the ends of the chain are approached [13].

The value of the plateau $O^\alpha \approx -0.3743$ ($\alpha = x, y, z$), the non-local order parameter for $S = 1$, was in accordance with earlier numerical simulations [29]. Figure 5 presents how the individual components of the non-local correlations change over time for various values of the uniaxial anisotropy.

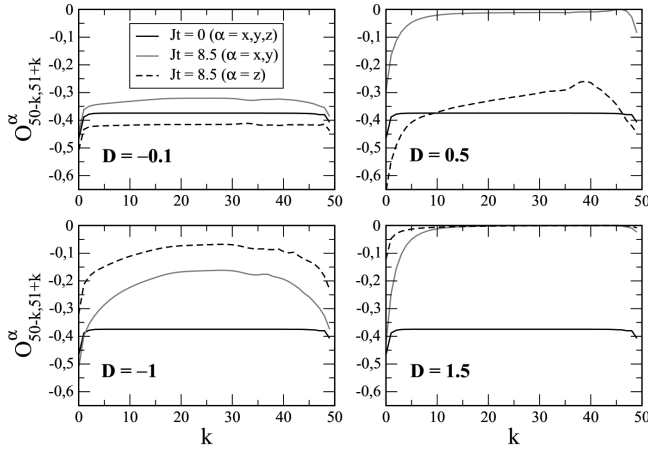


Fig. 5. The individual components of the non-local order parameter for various D at $Jt = 8.5$. At $t = 0$ the value of the plateau is $O^\alpha \approx -0.3743$. The figure includes cases related to the Haldane phase ($D/|J| = -0.1$ and 0.5), the Néel phase ($D/|J| = -1$) and large- D phase (1.5).

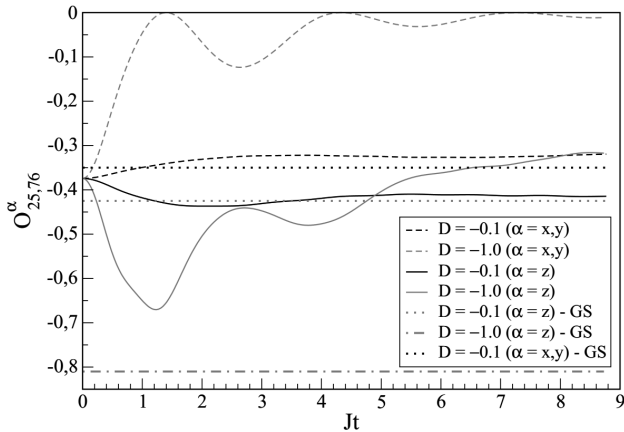


Fig. 6. The time dependence of the non-local order parameter between the S_{25}^α and S_{76}^α spins for various negative D . The figure includes cases related to the Haldane phase ($D/|J| = -0.1$), and the Néel phase ($D/|J| = -1$). The dotted lines correspond to the non-local order parameter for the ground state $|\phi_0\rangle$ of the anisotropic Hamiltonian. For $D/|J| = -1$ the non-local order parameter $O^{x,y}$ vanishes.

Figures 6 and 7 present the time evolution of the string correlation between the spins arranged symmetrically in the distance of 51 lattice constants. The string correlations calculated in the same way, for the ground state of the anisotropic Hamiltonian are represented by dashed lines. The values of the z -th component of the non-local

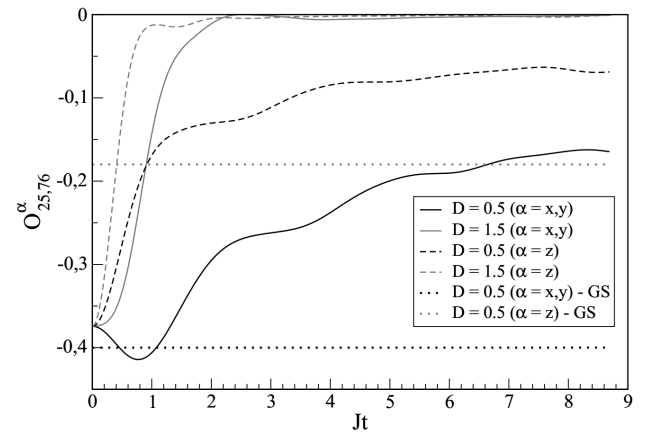


Fig. 7. The time dependence of the non-local order parameter between the S_{25}^α and S_{76}^α spins for various positive D . The figure includes the cases related to the Haldane phase ($D/|J| = 0.5$), and large- D phase ($D/|J| = 1.5$). The dotted lines correspond to the non-local order parameter for the ground state $|\phi_0\rangle$ of the anisotropic Hamiltonian. For $D/|J| = 1.5$ the non-local order parameters $O^{x,y}$ and O^z vanish.

order parameter are in agreement with earlier reported data [23].

According to our results, when turning on of the uniaxial anisotropy leaves the system in the Haldane phase, the non-local order parameter of the evolving state takes non-zero values. Moreover, $O^{x,y} > O^z$ in most of the phase and only in the vicinity of the second-order Ising transition between the Haldane and Néel phases the last inequality is reversed. This is due to the proximity of the Néel phase where the ground state exhibits a spontaneous staggered magnetization, $O^{x,y}$ disappears but O^z continues to grow there. In turn, all components of the non-local order parameter evaluate to zero in the large- D phase.

As far as the values of the string correlations in the ground state of the anisotropic Hamiltonian are concerned, it is hard to say that the string correlations of the evolving state converge to them. Only one can see that such a tendency appears at the very beginning of the time evolution, but then vanishes. Perhaps, by analogy with the revivals for the Loschmidt echo, this trend is back from time to time, when the evolving state approaches to the ground state $|\phi_0\rangle$ of the anisotropic Hamiltonian. Unfortunately, our calculations are time-consuming and we are not able to perform them enough long to test conclusively the supposition.

6. Conclusions

We have examined the ground-state response of the finite $S = 1$ antiferromagnetic Heisenberg chain after a sudden change of the uniaxial anisotropy. Depending on the value of the uniaxial anisotropy parameter, the calculations were derived within (or outside) the region where

the Haldane gap survives. We tackle the problem considering the time evolution of the system and applying the MPS framework.

An exact expression for the time evolution of the Loschmidt echo has been derived. It consists of a time-independent part supplemented by the superposition of cosine functions. The collapse and revival of the Loschmidt echo have been investigated as well.

When turning on of the uniaxial anisotropy leaves the system in the Haldane regime, the non-local order parameter decreases, but still takes a finite value during the time evolution. On the other hand, when the uniaxial anisotropy is so large that the ground state of the anisotropic Hamiltonian is no longer in the Haldane phase, the nonlocal order parameter of the evolving initial state tends towards zero.

References

- [1] H.A. Bethe, *Z. Phys.* **71**, 205 (1931).
- [2] M.T. Hutchings, G. Shirane, R.J. Birgeneau, S.L. Holt, *Phys. Rev. B* **5**, 1999 (1972).
- [3] F.D.M. Haldane, *Phys. Rev. Lett.* **50**, 1153 (1983); F.D.M. Haldane, *Phys. Lett. A* **93**, 464 (1983).
- [4] M. Lewenstein, A. Sanpera, V. Ahufinger, B. Damski, A. Sen(De), U. Sen, *Adv. Phys.* **56**, 243 (2007).
- [5] A. Barasiński, W. Leoński, T. Sowiński, *J. Opt. Soc. Am. B* **31**, 1845 (2014).
- [6] U. Dorner, P. Fedichev, D. Jaksch, M. Lewenstein, P. Zoller, *Phys. Rev. Lett.* **91**, 073601 (2003).
- [7] J.J. Garcia-Ripoll, M.A. Martin-Delgado, J.I. Cirac, *Phys. Rev. Lett.* **93**, 250405 (2004).
- [8] I. Cohen, A. Retzker, *Phys. Rev. Lett.* **112**, 040503 (2014).
- [9] I. Cohen, P. Richerme, Z.-X. Gong, C. Monroe, A. Retzker, *Phys. Rev. A* **92**, 012334 (2015).
- [10] I. Affleck, T. Kennedy, E.H. Lieb, H. Tasaki, *Phys. Rev. Lett.* **59**, 799 (1987).
- [11] S.R. White, D.A. Huse, *Phys. Rev. B* **48**, 3844 (1993).
- [12] D. Woźniak, A. Drzewiński, G. Kamieniarz, *Acta Phys. Pol. A* **127**, 333 (2015).
- [13] D. Woźniak, A. Drzewiński, G. Kamieniarz, *J. Appl. Math. Comput. Mech.* **13**, 151 (2014).
- [14] S. Ejima, H. Fehske, *Phys. Rev. B* **91**, 045121 (2015).
- [15] F. Pollmann, A.M. Turner, *Phys. Rev. B* **81**, 064439 (2010).
- [16] T. Senthil, A. Vishwanath, L. Balents, S. Sachdev, M.P.A. Fisher, *Science* **303**, 1490 (2004).
- [17] T. Kennedy, H. Tasaki, *Phys. Rev. B* **45**, 304 (1992); T. Kennedy, H. Tasaki, *Commun. Math. Phys.* **147**, 431 (1992).
- [18] M. den Nijs, K. Rommelse, *Phys. Rev. B* **40**, 4709 (1989).
- [19] A.F. Albuquerque, C.J. Hamer, J. Oitmaa, *Phys. Rev. B* **79**, 054412 (2009) and references therein.
- [20] M. Orendáč, A. Orendáčová, J. Černák, A. Feher, P.J.C. Signore, M.W. Meisel, S. Merah, M. Verdager, *Phys. Rev. B* **52**, 3435 (1995).
- [21] S. Chattopadhyay, D. Jain, V. Ganesan, S. Giri, S. Majumdar, *Phys. Rev. B* **82**, 094431 (2010).
- [22] Yu-Chin Tzeng, Min-Fong Yang, *Phys. Rev. A* **77**, 012311 (2008).
- [23] G. De Chiara, M. Lewenstein, A. Sanpera, *Phys. Rev. B* **84**, 054451 (2011).
- [24] L. Lepori, G. De Chiara, A. Sanpera, *Phys. Rev. B* **87**, 235107 (2013).
- [25] S. Hu, B. Normand, X. Wang, L. Yu, *Phys. Rev. B* **84**, 220402(R) (2011).
- [26] C. Rudowicz, *Physica B* **436**, 193 (2014).
- [27] G. De Chiara, L. Lepori, M. Lewenstein, A. Sanpera, *Phys. Rev. Lett.* **109**, 237208 (2012).
- [28] U. Schollwöck, *Rev. Mod. Phys.* **77**, 259 (2005); U. Schollwöck, *Ann. Phys.* **326**, 96 (2011).
- [29] F. Verstraete, K. Cirac, *Phys. Rev. B* **73**, 094423 (2006); F. Verstraete, V. Murg, K. Cirac, *Adv. Phys.* **57**, 143 (2008).
- [30] S. Östlund, S. Rommer, *Phys. Rev. Lett.* **75**, 3537 (1995).
- [31] D. Woźniak, A. Drzewiński, G. Kamieniarz, *Acta Phys. Superfic.* **12**, 187 (2012).
- [32] T. Gorin, T. Prosen, T.H. Seligman, M. Žnidarič, *Phys. Rep.* **435**, 33 (2006); E.V.H. Doggen, J.J. Kinnunen, *New J. Phys.* **16**, 113051 (2014) and references therein.
- [33] J. Eisert, M. Friesdorf, C. Gogolin, *Nature Phys.* **11**, 124 (2015).
- [34] A. Kowalewska-Kudłaszuk, J.K. Kalaga, W. Leoński, *Phys. Rev. E* **78**, 066219 (2008).
- [35] A. Kowalewska-Kudłaszuk, J.K. Kalaga, W. Leoński, V. Cao Long, *Phys. Lett. A* **376**, 1280 (2012).
- [36] A. Kowalewska-Kudłaszuk, J.K. Kalaga, W. Leoński, *Phys. Lett. A* **373**, 1334 (2009).
- [37] B. Pozsgay, *J. Stat. Mech.* **13**, P10028 (2013).
- [38] Y.S. Weinstein, S. Lloyd, C. Tsallis, *Phys. Rev. Lett.* **89**, 214101 (2002).
- [39] R. Dubertrand, A. Goussev, *Phys. Rev. E* **89**, 022915 (2014).